



**QUEEN'S
UNIVERSITY
BELFAST**

Mathematical modelling of quantum yield enhancements of methyl orange photooxidation in aqueous TiO₂ suspensions under controlled periodic UV LED illumination

Tokode, O., Prabhu, R., Lawton, L. A., & Robertson, P. K. J. (2014). Mathematical modelling of quantum yield enhancements of methyl orange photooxidation in aqueous TiO₂ suspensions under controlled periodic UV LED illumination. *Applied Catalysis B: Environmental*, 156-157, 398-403. <https://doi.org/10.1016/j.apcatb.2014.03.046>

Published in:

Applied Catalysis B: Environmental

Document Version:

Peer reviewed version

Queen's University Belfast - Research Portal:

[Link to publication record in Queen's University Belfast Research Portal](#)

Publisher rights

Copyright © 2014 Elsevier B.V.

This manuscript version is made available under the CC-BY-NC-ND 4.0 license <http://creativecommons.org/licenses/by-nc-nd/4.0/>, which permits distribution and reproduction for non-commercial purposes, provided the author and source are cited.

General rights

Copyright for the publications made accessible via the Queen's University Belfast Research Portal is retained by the author(s) and / or other copyright owners and it is a condition of accessing these publications that users recognise and abide by the legal requirements associated with these rights.

Take down policy

The Research Portal is Queen's institutional repository that provides access to Queen's research output. Every effort has been made to ensure that content in the Research Portal does not infringe any person's rights, or applicable UK laws. If you discover content in the Research Portal that you believe breaches copyright or violates any law, please contact openaccess@qub.ac.uk.

1 **Mathematical modelling of quantum yield enhancements of methyl**
2 **orange photooxidation in aqueous TiO₂ suspensions under**
3 **controlled periodic UV LED illumination**

4 Oluwatosin Tokode, Radhakrishna Prabhu, Linda A Lawton and Peter K. J.
5 Robertson*.

6 IDEaS, Innovation, Design and Sustainability Research Institute, Robert
7 Gordon University, Schoolhill, Aberdeen, AB10 1FR, UK.

8 **ABSTRACT**

9 Quantum yields of the photocatalytic degradation of methyl orange under
10 Controlled Periodic Illumination (CPI) have been modelled using existing
11 models. A modified Langmuir-Hinshelwood (L-H) rate equation was used to
12 predict the degradation reaction rates of methyl orange at various duty
13 cycles and a simple photocatalytic model was applied in modelling quantum
14 yield enhancement of the photocatalytic process due to the CPI effect. A
15 good agreement between the modelled and experimental data was
16 observed for quantum yield modelling. The modified L-H model, however,
17 did not accurately predict the photocatalytic decomposition of the dye under
18 periodic illumination.

19 **KEYWORDS**

20 Photocatalysis, Titanium dioxide, Quantum yield, Langmuir-Hinshelwood,
21 Mathematical model

22 *Corresponding author P.K.J. Robertson email: peter.robertson@rgu.ac.uk

1. INTRODUCTION

Semiconductor photocatalysis using titanium dioxide (TiO₂) photocatalysts is an active area of research in environmental remediation, which has been demonstrated to be effective in the destruction of a variety of environmental pollutants and toxins [1-5]. Photocatalytic detoxification takes place when redox reactions involving charge-carriers (e^-_{cb} and h^+_{vb}) are initiated by the absorption of photons of appropriate energy by the photocatalyst/substrate. If the initial photo-excitation takes place in the photocatalyst (TiO₂), which then transfers energy or an electron to the adsorbed ground state molecule (substrate), a sensitized photo-reaction is said to have taken place. When the reverse takes place, the process is referred to as a catalyzed photo-reaction [6]. Once generated, the fate of the electron-hole pair follows two notable pathways; charge-carrier recombination in the bulk or surface and charge transfer to adsorbed species (H₂O, OH⁻ and O₂) producing intermediate species (O₂⁻ and OH[•]). The generated h^+_{vb} and OH[•] having redox potentials of +2.53 and +2.27 respectively [7] at pH 7 are highly electropositive and responsible for the photooxidation of adsorbed substrates. Since charge-carrier recombination is a faster primary process than interfacial charge transfer [4], most electron-hole pairs recombine therefore limiting charge transfer which is necessary for initiating the redox reactions required for photocatalytic detoxification. Hence, charge-carrier recombination is the most important primary process limiting the efficiency of the photocatalytic process.

The efficiency of photocatalytic oxidation processes is measured as the rate of photocatalytic reaction per photon absorbed by the catalyst. This is the quantum yield (ϕ), which is directly proportional to the electron transfer rate constant (k_t) and inversely proportional to the charge carrier recombination rate constant (k_r) (1).

$$\phi \propto k_t \propto 1/k_r \quad (1)$$

In the absence of charge-carrier recombination, the quantum yield, ϕ of an ideal photocatalytic system will be unity (2). k_t will depend on migration of charge carriers to the surface and the equalization of electron-hole

55 concentration such that $e^-_{cb} = h^+_{vb}$ at the photocatalyst surface. In real
56 photocatalytic systems, however, $e^-_{cb} \neq h^+_{vb}$ at the surface.

57
$$\phi \propto k_t / (k_t + k_r) \quad (2)$$

58 In dilute aqueous solutions, ϕ is typically below 10% [8] whereas in the gas
59 phase ϕ exceeds 50% under low intensity illumination [9]. These low
60 quantum yields of TiO_2 photocatalytic oxidation prevent its application in
61 large scale water remediation [10]. Determination of ϕ for heterogeneous
62 photocatalysis is a difficult process because of the effects of scattering and
63 reflection of photons by the photocatalyst surface. Therefore, an alternative
64 measure of photocatalytic efficiency which is the photonic efficiency (ζ) can
65 be employed. Photonic efficiency takes into account the number of incident
66 photons and as a result, the measured efficiency is a lower limit of the ϕ
67 for any photocatalytic reaction because of the greater magnitude of photons
68 incident compared with photons absorbed [11].

69 In order to suppress charge-carrier recombination and enhance the
70 efficiency of photocatalytic oxidation Sczechowski et al. [12] suggested the
71 use of controlled periodic (transient) illumination as a means of increasing
72 the efficient use of photons in photocatalysis hence, increasing quantum
73 yield. Controlled periodic illumination (CPI) consist of a series of alternate
74 light and dark periods ($t_{\text{light}}/t_{\text{dark}}$) and is based on a hypothesis that
75 continuous introduction of photons may result in the build-up of charges
76 and photogenerated intermediates such as O^-_2 and OH^\bullet . These species take
77 part in the necessary redox reactions but can also participate in reactions
78 that favour charge-carrier recombination therefore; periodically illuminating
79 the TiO_2 particle at short intervals would inhibit the build-up of these species
80 and promote the favourable oxidation process.

81 Previous studies have shown that at equivalent average photon
82 absorption/flux, ϕ/ζ under periodic illumination do not exceed those under
83 continuous illumination [8]. In a more recent study [13], we showed
84 experimentally that the duty cycle (γ) and not the pulse width is responsible
85 for the increase in efficiency of photocatalysis under CPI. In this study, we
86 reproduce the results of our previous experimental study theoretically,

87 using existing CPI models. The reaction rates at various γ are calculated
88 using the modified Langmuir-Hinshelwood rate equation by Chen et al. [14]
89 and ϕ is calculated using the mathematical model developed by Upadhya
90 and Ollis [15].
91

2. MATHEMATICAL MODELS

2.1. Reaction rate modelling

For the modelling of photocatalytic reaction rates of methyl orange under CPI, the Langmuir-Hinshelwood (L-H) rate equation (3) was adopted. The L-H rate model is the simplest model consistent with Langmuir's equilibrium isotherm and is widely applied to photocatalytic reactions [16-18]. The model interprets the photocatalytic rate of reaction, r as a product of the reaction rate constant, k_r of surface species (photogenerated and substrate) and the extent of substrate adsorption, K_{ads} . Competition for adsorption by other species is represented by adding the terms $K_{ads}C$ to the denominator.

$$- \delta C / \delta t = r = k_r K_{ads} C / (1 + K_{ads} C) \quad (3)$$

Where the rate r is taken as an initial rate r_0 , C is taken as the equilibrium concentration C_e , k_r is the reaction rate constant under experimental conditions and K_{ads} is the Langmuir adsorption coefficient. However, not all experimental data on photocatalytic reactions can be predicted by this model [2, 19]. The model is best applied to reactions that follow the pathway of; (i) adsorption of reacting species on the catalyst surface, (ii) reaction involving adsorbed species, (iii) desorption of reaction products.

Chen et al. in the decomposition of *o*-cresol under controlled periodic illumination (CPI) modified the model by incorporating the parameters, which account for the pulsing effect of reactions under CPI [14]. The reaction was assumed to take place on the outer surface of the TiO_2 particle and for a photoreactor under periodic illumination, the average light intensity and order of light intensity were incorporated into the rate equation (4) as follows:

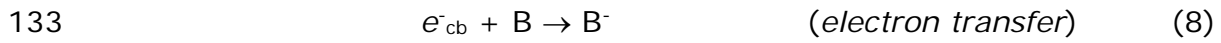
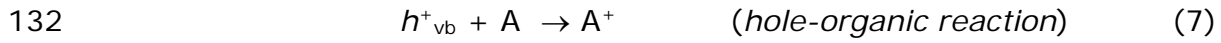
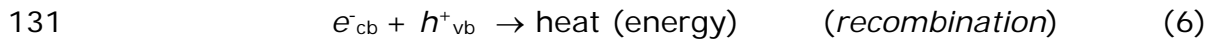
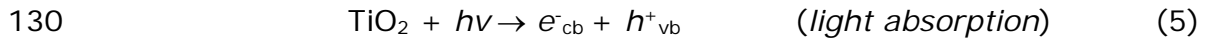
$$- \delta C / \delta t = r_0 = k_r (\gamma I_{max})^m K_{ads} C_e / (1 + K_{ads} C_e) \quad (4)$$

Where $\gamma = [t_{light} / (t_{light} + t_{dark})]$ is the duty cycle of UV illumination and is defined as the ratio of the total illumination period to the total operating period; a duty cycle of 0.5 or 50% means the lights are on 50% of the time, I_{max} is the light intensity ($I_{avg} = \gamma I_{max}$) and m is the order of light intensity.

123

124 2.2. Quantum yield modelling

125 Upadhyaya and Ollis [15] proposed a transient kinetic model to show rapid
 126 photooxidation of surface reactants by the oxidizing species (h^+_{vb}) accounts
 127 for high efficiencies in CPI experiments. The model formulation assumed
 128 the entire photocatalytic process to occur on a single TiO_2 particle. The
 129 factors affecting quantum yield are summarised in the following reactions:



134 The quantum yield, Φ , of the organic substrate was defined as an integral
 135 of the instantaneous quantum yield over time;

$$136 \quad \Phi = \int k_1(h^+(t))\Omega_A(t) \delta t / \int k_g I \delta t \quad (9)$$

137 Where k_1 is the oxidation reaction rate constant, h^+ is the hole
 138 concentration, Ω_A is the surface fractional coverage of organic substrate, k_g
 139 is the light absorption rate constant and I is the incident light intensity. A
 140 high quantum yield will be characterized by a high h^+ and total surface
 141 coverage of the TiO_2 particle with reactants. Light and dark periods are
 142 incorporated for a TiO_2 particle under periodic illumination and the resultant
 143 quantum yield is given as:

$$144 \quad \Phi_{\text{periodic}} = \int^{t_{\text{light}} + t_{\text{dark}}} k_1 n_A(h^+(t))\Omega_A(t) \delta t / \int^{t_{\text{light}}} k_g I \delta t \quad (10)$$

$$145 \quad \Phi_{\text{continuous}} = \int^{t_{\text{light}}} k_1 n_A(h^+)_{ss} \Omega_{Ass} \delta t / \int^{t_{\text{light}}} k_g I \delta t \quad (11)$$

146 Where n_A is the number of surface sites for organic substrate, t_{light} is the
 147 light time, t_{dark} is the dark time. The period for the periodic illumination was

kept constant at 1 s for different γ from $0 < \gamma \leq 1$. Hole concentration is a function of time and is described by eq. (12).

$$\delta(h^+)/\delta t = k_g I - k_r(h^+)(e^-) - k_1(h^+)n_A\Omega_A \quad (12)$$

2.3. Base case parameter values

The same values adopted from the literature by Upadhyaya and Ollis [15] were used for the constants and parameters in the study. In order to solve (12), a steady state approximation was adopted for electron concentration. It was calculated from typical values of h^+ quantum yields [20] with the assumption that equal number of holes and electrons are generated. Surface fractional coverage was taken to be constant, and assumed to equal $7 \times 10^{12} \text{ cm}^{-2}$. Furthermore it is assumed that 50 photons are absorbed in t_{light} of 1 s.

3. Methodology for quantum yield modelling

The data used in the quantum yield modelling investigated in this study were obtained from experiments carried out in a previous study [13] where three sets of experiments were carried out to investigate the effect of the period, t_{light} and t_{dark} on the photonic efficiency of the photocatalytic degradation of methyl orange under low intensity UV light. The experiments were designed using a controlled experimental approach (Table 1.) in order to increase confidence in the outcome of the study.

Table 1.

The photonic efficiency remained as the dependent variable throughout the different sets of experiments while the period, t_{light} and t_{dark} each served as controlled variables in one set, and independent variable in other sets of experiments, hence providing a critical evaluation of their effects on photonic efficiency. The photonic efficiency, ζ of the photocatalytic degradation process was calculated as the rate of reaction of the photocatalytic degradation divided by the incident photon rate [21, 22].

$$\zeta = \frac{\text{Reaction rate (M s}^{-1}\text{)}}{\text{Incident photon rate (M s}^{-1}\text{)}} \quad (13)$$

The reaction rate, r was calculated as change in concentration with time,

$$r = \frac{C_2 - C_1}{\text{Time}} \quad (14)$$

where C_1 is the concentration at the start of illumination and C_2 is the final concentration while the incident photon rate from the UV LEDs determined by the ratio of the total energy of the LEDs to the energy of a single photon was calculated to be 4.85×10^{-8} einsteins $L^{-1} s^{-1}$.

Photonic efficiencies were determined in the experimental study because incident photons were taken into consideration while quantum yields were determined for the theoretical study because the formulation of the mathematical model used was based on photon absorption by the TiO_2 catalyst [15]. Hence, in this study, photonic efficiency values are reported for the experimental investigation of methyl orange photooxidation while quantum yield values are reported for the results of the theoretical study. Both results are presented in figures for evaluation of the mathematical model. The data for the experimental determination of ζ in the experimental study showing the values of γ , t_{light} and t_{dark} is given in table 2. The same data was also used in the modelling of ϕ as carried out in the study.

Table 2.

4. RESULTS AND DISCUSSION

3.1. Photocatalytic rate modelling

The experimental data showed the effect of γ on photocatalytic degradation rates of methyl orange. A 5 g/L loading of TiO_2 was suspended in 100 mL methyl orange solution in distilled water with an initial concentration of 2.5×10^{-2} mM. The photocatalytic degradation of methyl orange solution was carried out over a period of 170 min including 30 min of dark adsorption which was experimentally determined as the time taken for adsorption equilibrium. Methyl orange photooxidation proceeds by surface-trapped holes which are indistinguishable from OH^\bullet radicals adsorbed on the surface of the hydroxylated TiO_2 particle resulting in $\{\text{Ti}^{\text{IV}}\text{OH}^\bullet\}^+_{\text{ads}}$ which is readily available for oxidative reactions with the surface adsorbed methyl orange [23, 24]. The same experimental condition was used for all values of γ , the period ($t_{\text{light}} + t_{\text{dark}}$) was kept constant while t_{light} and t_{dark} were varied. The reaction order n varied with γ (Table 3.), I_{max} was $< 200 \text{ Wm}^{-2}$ therefore m was taken to be first-order [25]. K_{ads} and k_r were obtained from the plot of $1/r_0$ against $1/\gamma$, the intercept was equal to $1/k_r$ while the slope provided the solution for $1/k_r K_{\text{ads}}$ hence, the values of K_{ads} and k_r were $0.645 \text{ dm}^3\text{mol}^{-1}$ and $4.85 \times 10^{-4} \text{ mMmin}^{-1}$ or min^{-1} with respect to the reaction order.

Table 3.

An increase in photocatalytic rates was observed with increasing γ for the experimental and model data (fig. 1). This is because of an increase in the average intensity of illumination. Generally for photocatalytic reactions, a linear relationship exists between photooxidation rates and light intensity at low light intensities. The relationship tends towards a square root relationship as intensity increases and eventually rate becomes independent of intensity at very high intensities [26]. The experimental results however showed a significantly different trend to that obtained with the model. The experimental data exhibited a non-linear trend while the model followed a linear trend. Also, there was a significant difference in the order of magnitude of the determined rates of reaction and this resulted in a poor fit of the experimental data by the model.

Figure 1.

Chen et al. who developed and first reported the use of this model reported a good fit to the experimental rates [14]. Their plot involved reaction rates at several concentrations and a single γ . Our experiments monitored reaction rates at a single concentration but several γ . The varying I_{avg} as a result of changing γ had a significant influence on the model rates and this accounted for the significant disagreement between the model and experimental rates in trend and magnitude. Photocatalytic reactions under periodic illumination involve complex transient mechanisms therefore developing a model for the dependence of the reaction rate on the experimental parameters over the reaction time can be difficult. The dependence of the constants K_{ads} and k_r on the intensity of UV illumination is well established (15,16) [27-30] and this is not accounted for in the modified L-H model.

$$K_{\text{ads}} \propto 1/\gamma I_{\text{max}} \quad (15)$$

$$k_r \propto \gamma I_{\text{max}} \quad (16)$$

The variation of the constants K_{ads} and k_r with UV intensity implies their values when obtained from a plot of $1/r_0$ against $1/\gamma$ will not give a truly representative value for each γ in the modified L-H model. Furthermore, orders of reaction rate dependence on photon flux and reagent concentration are independent of each other [31]. This presents a problem for the model as reaction order with respect to concentration changes with an effect on k_r while order of photon flux remains the same.

3.2. Quantum yield modelling

The quantum yield modelling of the photocatalytic degradation of methyl orange confirmed the same trends from experimental data which were previously reported in the literature [13]. The effect of a constant period and varying t_{light} and t_{dark} on the quantum yield was modelled (fig. 2). All events required for photocatalytic oxidation (5-8) were constrained in 1 s such that $t_{\text{light}} + t_{\text{dark}} = 1$ s for all duty cycles.

Figure 2.

A general increase in quantum yield as duty cycle decreased was observed indicating an inverse relationship between ϕ and γ . Quantum yield and photonic efficiency differ because of the difference in accounting for photons, ϕ takes into account the amount of photons absorbed by the catalyst and this is affected by, reflection, transmission and scattering which is significant and can vary as much as 13% - 76% depending on experimental conditions [32]. Photonic efficiency on the other hand takes into consideration only the incident photons on the photocatalyst, assuming all photons are absorbed and light-losses are negligible.

The model agreement with the experimental data in the modelling of the effect of t_{light} and t_{dark} on ϕ followed a similar trend. When t_{light} was kept constant while t_{dark} varied, the contributing effect of t_{dark} to quantum yield was observed. The approach taken involved the light time events mainly (5) taking place within 1 s therefore having a controlled impact on ϕ while the dark time events were varied by increasing t_{dark} from 0.1 s to 1 s, the resulting range for the duty cycle was $\gamma = 0.39 - 0.91$ (fig. 3).

Figure 3.

The dark period is devoted to the replenishment of surface adsorbed species by the transfer of electrons to adsorbed oxygen (8) and/or the adsorption of oxygen onto the surface. Consequently, a higher rate constant for these steps will result in higher quantum yields. Figure 3 shows the relatively small improvements in quantum yield as t_{dark} increases in agreement with previous experimental results. The resulting increase in quantum yield was inferior to the same effect produced by an increasing t_{light} . This is as a result of the sensitivity of the dark period to the rate-limiting nature of (8) [15, 33].

In the third modelling result, the experimental light time was varied while the dark time was kept constant. This produced the effect of an increase in I_{avg} and higher photon absorption by the photocatalyst as t_{light} increased, without a corresponding increase in t_{dark} . The modelled results (fig. 4) show the quantum yield improved with decreasing duty cycle.

Figure 4.

As t_{light} increased, more time was available for (5), which is the first step in the photocatalytic process, giving rise to (6) resulting in a decrease in quantum yield. The modelling further reiterates our previous findings which show that decreasing t_{light} at constant t_{dark} has a greater effect on quantum yield than increasing t_{dark} at constant t_{light} or varying both alternatively by varying the period.

The enhancement observed in the mathematical modelling of ϕ when controlled periodic illumination is employed is produced by the duty cycle, γ , which is a function of t_{light} and t_{dark} therefore, their alternating effects contribute to the overall quantum yield enhancement. Figure 5 shows the overall trend of quantum yield enhancement as a result of reducing duty cycle using modelled data. This is in agreement with the result using experimental data [13] depicting a trend of increasing quantum yield as duty cycle decreases irrespective of t_{light} and t_{dark} .

Figure 5.

5. Conclusion

Several mathematical models exist for photocatalytic reactions using TiO_2 with light intensity distribution and reactor modelling receiving the most attention. The modified L-H rate equation used in the study is the most suitable for modelling photocatalytic reaction rates under controlled periodic illumination because of the integration of I_{max} , m and γ which account for the UV intensity, order of intensity and periodicity of illumination respectively. The influence of γ on the reaction order and the variation of the constants K_{ads} and k_r with UV intensity, however, makes the model suitable only for reactions with a single γ . The quantum yield model although speculative, gives a good agreement between the trends for the experimental data and model data. This suggests a potential for the formulation of more detailed models which provide a thorough understanding of the CPI effect and the modelling of photocatalytic rates under controlled periodic illumination in the aqueous phase.

Acknowledgement

The authors would like to thank the Scottish Funding Council who funded R. Prabhu's lectureship through the Northern Research Partnership's research pooling initiative in engineering.

328	Nomenclature	
329	C	Concentration
330	C_1	Initial concentration
331	C_2	Final concentration
332	C_e	Equilibrium concentration
333	k_r	Reaction rate constant
334	k_1	Oxidation reaction rate constant
335	K_{ads}	Langmuir adsorption coefficient
336	k_g	Light absorption rate constant
337	I_{avg}	Average intensity
338	I_{max}	Maximum intensity
339	I	Incident light intensity
340	m	Order of light intensity
341	n	Order of reaction
342	n_A	Number of surface sites for MO
343	r_0	Initial reaction rate
344	r	Reaction rate
345	t	Time
346	t_{dark}	Dark time
347	t_{light}	Light time
348	t_{total}	Total time
349	Ω_A	Surface fractional coverage by MO

350	h^+	Hole concentration
351	e^-	Electron concentration
352	k_t	Electron transfer rate constant
353	e^-_{cb}	Conduction band electron
354	h^+_{vb}	Valence band holes
355	<i>Greek letters</i>	
356	γ	Duty cycle
357	ϕ	Quantum yield
358	ζ	Photonic efficiency
359	<i>Abbreviations</i>	
360	MO	Methyl orange
361	CPI	Controlled Periodic Illumination
362	L-H	Langmuir-Hinshelwood
363		

364 **References**

- 365 [1] P.K.J. Robertson, D.W. Bahnemann, J.M.C. Robertson, F. Wood, in: P.
 366 Boule, D.W. Bahnemann, P. K. J. Robertson (Eds.), *Environmental*
 367 *Photochemistry Part II*, Springer-Verlag Berlin Heidelberg. (2005, pp.)
 368 367-424.
- 369 [2] P.K.J. Robertson, L.A. Lawton, B. Munch, J. Rouzade, *Chem. Commun.*
 370 (1997) 393-394.
- 371 [3] A. Mills, S. Le Hunte, *J. Photochem. Photobiol. A.* 108 (1997) 1-35.
- 372 [4] M.R. Hoffmann, T.S. Martin, W. Choi, W.D. Bahnemann, *Chem. Rev.*
 373 95 (1995) 69-96.
- 374 [5] D. Bahnemann, D. Bockelmann, R. Goslich, *Sol. Energ. Mater.* 24
 375 (1991) 564-583.
- 376 [6] L.A. Linsebigler, G. Lu , T.J. Yates, *Chem. Rev.* 95 (1995) 735-758.
- 377 [7] A. Fujishima, T.N. Rao, D.A. Tryk, *J. Photochem. Photobiol. C:*
 378 *Photochemistry Reviews.* 1 (2000) 1-21.
- 379 [8] J.G.C. Cornu, A.J. Colussi, M.R. Hoffmann, *J. Phys. Chem. B.* 105
 380 (2001) 1351-1354.
- 381 [9] Y. Ohko, K. Hashimoto, A. Fujishima, *J. Phys. Chem. A.* 101 (1997)
 382 8057-8062.
- 383 [10] D. Bahnemann, J. Cunningham, M.A. Fox, E. Pelizzetti, P. Pichat, N.
 384 Serpone, in: *Aquatic and Surface Photochemistry*. D. Crosby, G. Helz, R.
 385 Zepp (Eds.). Lewis, Boca Raton, FL. (1994) pp. 261–316,
- 386 [11] N. Serpone, *J. Photochem. Photobiol. A.* 104 (1997) 1-12.
- 387 [12] J.G. Sczechowski, C.A. Koval, R.D. Noble, *J. Photochem. Photobiol. A.*
 388 74 (1993) 273-278.
- 389 [13] O. Tokode, R. Prabhu, L.A. Lawton, P.K.J. Robertson, *J. Catal.* 290
 390 (2012) 138-142.
- 391 [14] H. Chen, Y. Ku, A. Irawan, *Chemosphere.* 69 (2007) 184-190.
- 392 [15] S. Upadhyay, F.D. Ollis, *J. Phys. Chem. B.* 101 (1997) 2625-2631.
- 393 [16] K.V. Kumar, K. Porkodi, F. Rocha, *Catal. Commun.* 9 (2008) 82-84.
- 394 [17] A. Mills, J. Wang, D.F. Ollis, *J. Catal.* 243 (2006) 1-6.
- 395 [18] D. Ollis, *Top. Catal.* 35 (2005) 217-223.

396 [19] S. Valencia, F. Catano, L. Rios, G. Restrepo, J. Marín, Appl. Catal. B-
397 Environ. 104 (2011) 300-304.

398 [20] K. Ishibashi, A. Fujishima, T. Watanabe, K. Hashimoto, J.
399 Photochem. Photobiol. A. 134 (2000) 139-142.

400 [21] S. Sakthivel, M.V. Shankar, M. Palanichamy, B. Arabindoo, D.W.
401 Bahnemann, V. Murugesan, Water Res. 38 (2004) 3001-3008.

402 [22] J. Marugán, D. Hufschmidt, G. Sagawe, V. Selzer, D. Bahnemann,
403 Water Res. 40 (2006) 833-839.

404 [23] O. Tokode, R. Prabhu, L.A. Lawton, P.K.J. Robertson. The effect of pH
405 on the photonic efficiency of the destruction of methyl orange under
406 controlled under periodic illumination with UV-LED sources. Chem. Eng. J.
407 (2014), accepted for publication.

408 [24] D. Lawless, N. Serpone, D. Meisel, J. Phys. Chem. 95 (1991) 5166–
409 5170.

410 [25] I.K. Konstantinou, T.A. Albanis, Appl. Catal. B-Environ. 49 (2004) 1-
411 14.

412 [26] F.D. Ollis, E. Pelizzetti, N. Serpone, Environ. Sci. Technol. 25 (1991)
413 1522-1529.

414 [27] D.F. Ollis, J. Phys. Chem. B. 109 (2005) 2439-2444.

415 [28] Y. Xu, C.H. Langford, J. Photochem. Photobiol. A. 133 (2000) 67-71.

416 [29] A.V. Emeline, V. Ryabchuk, N. Serpone, J. Photochem. Photobiol. A.
417 133 (2000) 89-97.

418 [30] Y.R. Smith, A. Kar, V. Subramanian, Ind. Eng. Chem. Res. 48 (2009)
419 10268-10276.

420 [31] A. Emeline, A. Rudakova, V. Ryabchuk, N. Serpone, J. Phys. Chem.
421 B. 102 (1998) 10906-10916.

422 [32] A. Salinaro, A.V. Emeline, J. Zhao, H. Hidaka, V.K. Ryabchuk, N.
423 Serpone, Pure Appl. Chem. 71 (1999) 321-335.

424 [33] H. Gerischer, A. Heller, J. Electrochem. Soc. 139 (1992) 113-118.

425

426 **Captions for Tables**

427 Table 1: Controlled experimental approach used in obtaining experimental
428 data for quantum yield modelling.

429 Table 2: Values of γ , t_{light} and t_{dark} used for theoretical modelling of ϕ .

430 Table 3: Experimental conditions for methyl orange photooxidation rate
431 under controlled periodic illumination.

432

433

434
435
436
437

EXPERIMENT	DEPENDENT VARIABLE	INDEPENDENT VARIABLE	CONTROLLED VARIABLE
1	Photonic Efficiency	$t_{\text{light}} / t_{\text{dark}}$	Period
2	Photonic Efficiency	$t_{\text{dark}} / \text{Period}$	t_{light}
3	Photonic Efficiency	$t_{\text{light}} / \text{Period}$	t_{dark}

438
439
440

441 Table 1.

442
443
444

445

Varying Period			Varying t_{light}			Varying t_{dark}		
γ	$t_{\text{light}} \text{ (S)}$	$t_{\text{dark}} \text{ (S)}$	γ	$t_{\text{light}} \text{ (S)}$	$t_{\text{dark}} \text{ (S)}$	γ	$t_{\text{light}} \text{ (S)}$	$t_{\text{dark}} \text{ (S)}$
0.07	0.07	0.90	0.08	0.1	1.0	0.39	1.0	1.7
0.12	0.12	0.86	0.21	0.3	1.0	0.44	1.0	1.4
0.24	0.23	0.74	0.31	0.5	1.0	0.50	1.0	1.1
0.36	0.35	0.62	0.39	0.7	1.0	0.59	1.0	0.7
0.49	0.47	0.50	0.50	1.1	1.0	0.67	1.0	0.5
0.61	0.59	0.38				0.77	1.0	0.3
0.73	0.71	0.27				0.91	1.0	0.1
0.85	0.83	0.15						
1.0	-	-						

446

447 Table 2.

448

449
450
451
452
453
454

γ	I_{avg} (Wm ⁻²)	r_{40} (mMmin ⁻¹)	n
0.07	0.13	2.38E-05	0
0.12	0.21	2.50E-05	0
0.24	0.43	7.50E-05	0
0.36	0.64	1.00E-04	0
0.49	0.87	1.25E-04	0
0.61	1.09	1.50E-04	1
0.73	1.30	1.75E-04	1
0.85	1.51	1.85E-04	1
1.00	1.78	2.11E-04	1

455

456 Table 3.

457

Captions for figures

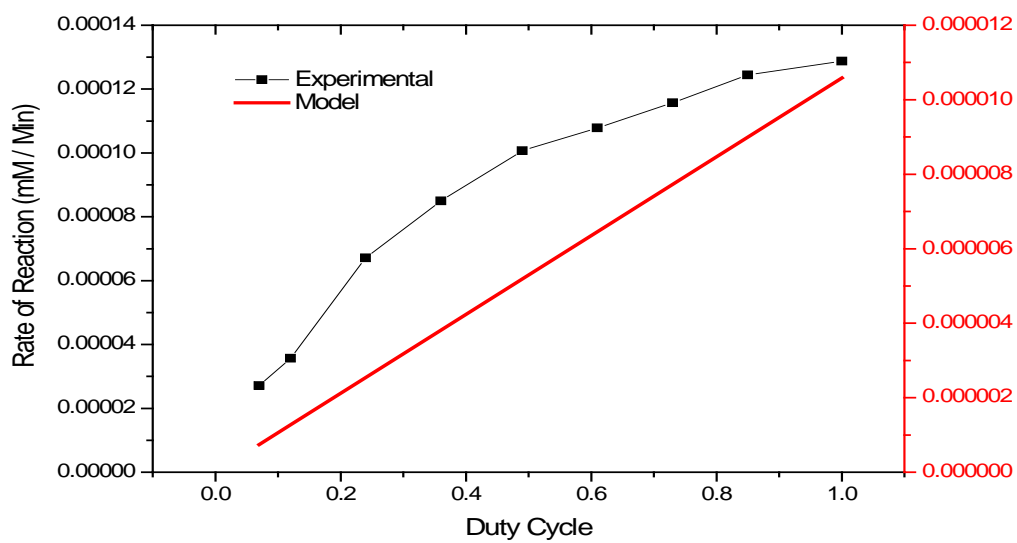
Figure 1: Correlation of modified L-H model data with experimental for methyl orange degradation rates at different γ .

Figure 2: Decreasing duty cycle resulting in a corresponding rise in quantum yield and photonic efficiency.

Figure 3: Contributing effect of t_{dark} to quantum yield enhancement

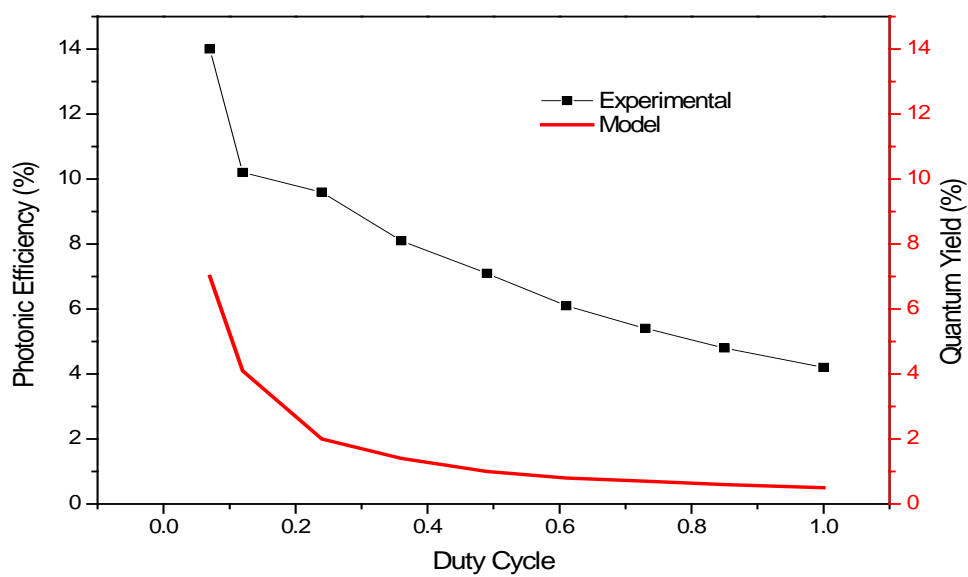
Figure 4: Contributing effect of t_{light} to quantum yield enhancement.

Figure 5: Overall quantum yield trend as a function of duty cycle with experimental result graph as an insert.



468

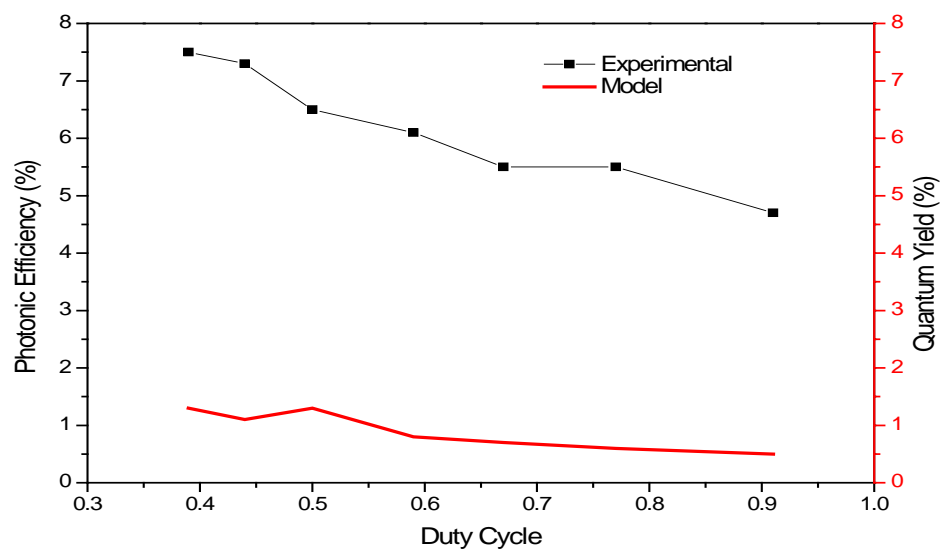
469 Figure 1.



470

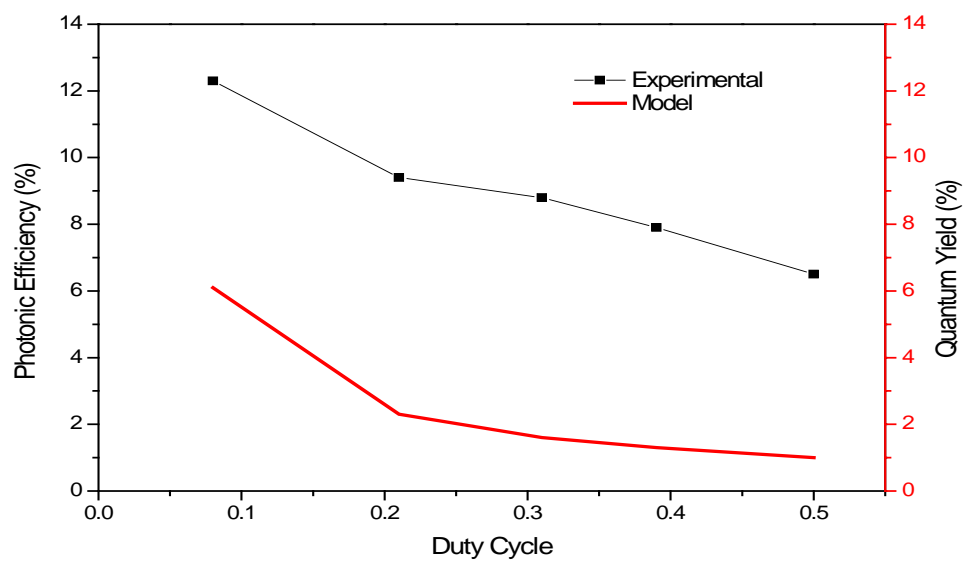
471 Figure 2.

472



473

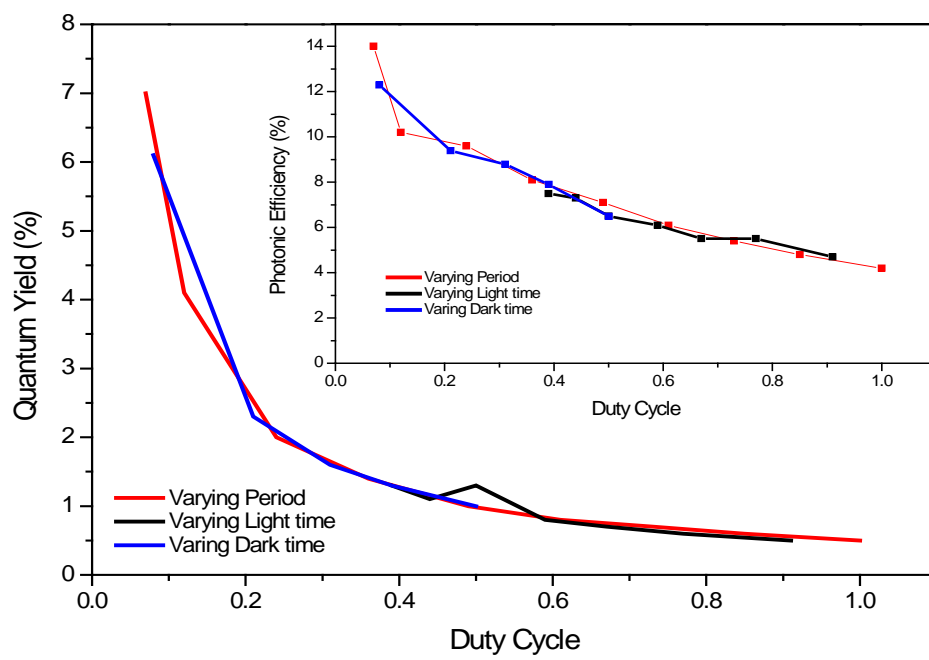
474 Figure 3.



475

476 Figure 4.

477



478

479 Figure 5.